IL NUOVO CIMENTO **38 C** (2015) 198
DOI 10.1393/ncc/i2015-15198-6

COLLOQUIA: LaThuile15

Light New Physics searches with BaBar

A. LUSIANI on behalf of the BaBar COLLABORATION
Scuola Normale Superiore and INFN, Sezione di Pisa - Pisa, Italy

received 2 October 2015

Summary. — Several hypothetical light New Physics particles have been searched using the clean and large electron-positron collision samples collected by the BaBar collaboration around the $\Upsilon(4S)$ resonance. No evidence has been found and 90% confidence level upper limits have been set on a dark photon decaying into electron or muon pairs, on a next-to-minimal supersymmetric Higgs boson decaying to charmed hadrons, and to an exotic π^0-like particle that would couple to the tau lepton.

PACS 12.60.Jv – Supersymmetric models.
PACS 13.20.Gd – Decays of J/Ψ, Υ, and other quarkonia.
PACS 13.66.Hk – Production of non-standard model particles in ee+ interactions.
PACS 14.80.Da – Supersymmetric Higgs bosons.

1. – Introduction

Well motivated New Physics (NP) models predict the existence of several new particles that are not yet excluded by experiment. The *BABAR* experiment has collected large samples of clean e^+e^- collisions with a general purpose full solid angle detector at and around the $\Upsilon(4S)$ on the PEP-II storage ring at the SLAC National Laboratory. This data sample is well suited to search for kinematically allowed NP particles that are rarely produced and may have escaped previous searches. The results of recent searches for NP light particles with *BABAR* are reported in the following.

2. – Search for Dark Photon into e^+e^- or $\mu^+\mu^-$

Light NP particles may be loosely coupled with ordinary matter through "portals" [1], which provide interactions between the Standard Model (SM) fields and "dark" fields, which can be scalar, pseudoscalar, vector or spin-1/2 fermions. A model for weakly interacting Dark Matter particles predicts [2] the existence of a "Dark Photon" A' with mass around 1 GeV, which interacts with the SM particles via a "kinetic mixing" term $\Delta\mathcal{L} = (\epsilon/2)F^{Y,\mu\nu}F'_{\mu\nu}$, with a coupling constant $\epsilon \ll 1$.

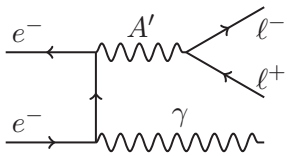

Fig. 1. – Diagram for $e^+e^- \to \gamma A' \to \gamma\ell^+\ell^-$.

A search for A' production in the process $e^+e^- \to \gamma A' \to \gamma\ell^+\ell^-$ ($\ell^\pm = e^\pm$ or $\mu^\pm$ (fig. 1) has been conducted on the whole *BABAR* data sample of $514\,\mathrm{fb}^{-1}$ [3]. The A' branching ratios into $\ell^+\ell^-$ are expected to be sizeable over the whole hypothetical mass range [4] (see also fig. 2). With respect to the process $e^+e^- \to \gamma\gamma$, the cross-section for this process is reduced by a factor ϵ^2.

We select events with a final state containing two oppositely-charged leptons and a photon and do a kinematic fit of the reconstructed track parameters to match the center-of-mass (CM) energy assuming all tracks come from the interaction point (IP). We suppress background removing events consistent with having an electron conversions and requiring a good-quality photon. According to simulation, which is consistent with the data, the selection efficiency is typically 15% (35%) for the electron pair (muon pair) channel.

We search for a signal peak on top of a smooth background in the lepton pair invariant mass, which is fitted from the sidebands. Therefore, we do not need to accurately simulate the SM expected candidates yield. We nevertheless perform a Monte Carlo (MC) simulation and verify that the simulation is reasonably accurate except the m_{ee} low-mass region, where radiative Bhabha simulation is known to be relatively less reliable. Further details are in the *BABAR* publication [3]. In order to get a smoother behaviour at threshold, we consider for muons the reduced mass $m_R = \sqrt{(m^2_{\mu\mu} - 4m^2_\mu)}$ rather than the invariant mass. Figure 3 shows the mass and reduced mass distributions in data and simulation.

We fit for a signal peak with a mass-dependent shape, interpolated from simulation and tuned using known resonances fitted on data. We scan the electron and muon

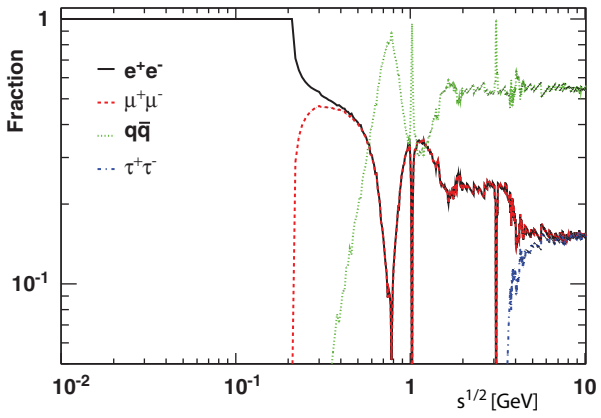

Fig. 2. – Branching fraction predictions for $A' \to \ell^+\ell^-$ and $A' \to q\bar{q}$ as a function of $m_{A'}$ [4].

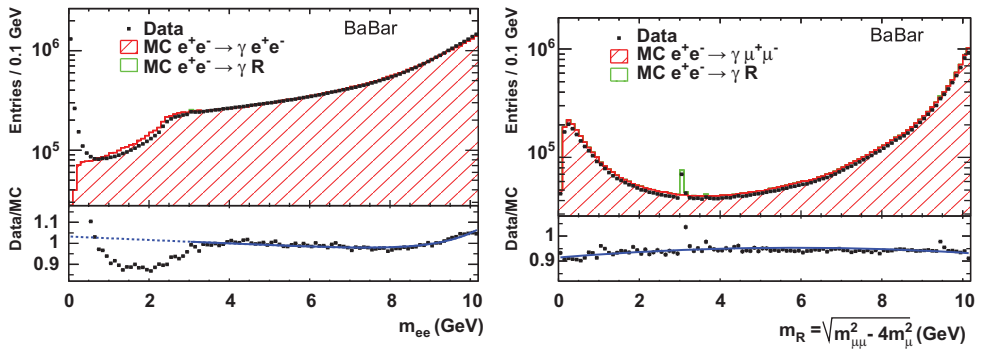

Fig. 3. – Electron pair mass spectrum (left) and muon pair reduced mass spectrum (right) for data and simulation. On the bottom the data/simulation ratio is reported.

pairs mass distributions with approximately 5500 steps, with sizes about half the mass resolution. At each mass point m, we perform a fit on a mass interval sized to about 20–30 times the mass resolution, using a likelihood function describing the signal peak centered on m over a polynomial background. The scan is not performed in the vicinity of known resonances [ω, ϕ, J/ψ, $\psi(2S)$, $\Upsilon(1S, 2S)$]. Rather, each resonance is fitted on data, and the resonance tails are added to the likelihood in addition to the signal and non-peaking background components. For the ω and ϕ resonances, their interference with the non-resonant channel is also modelled and used in the maximum likelihood fit.

In the fit, the signal component can be negative, but the probability is constrained to be non-negative. We determine the significance of each fit as $S = \sqrt{2\log(L/L_0)}$, where L and L_0 are the maximum-likelihood values for fits with and without freely varying signal, respectively. We estimate the significance of the whole scan by estimating the trial factors with a large sample of simulated Monte Carlo experiments. The largest local significance is 3.4σ (2.9σ) for electron pairs (muon pairs), corresponding to a global significance of 0.57 (0.94), consistent with the background-only hypothesis.

In absence of signal evidence, we compute a 90% confidence level (CL) Bayesian upper limit on the cross-section $e^+e^- \to \gamma A'$, combining both channels. The determination uses the *BABAR* luminosity (with ∼0.6% uncertainty), the estimated efficiency (with 0.5–4% uncertainty) and the predicted branching fractions in ref. [4] (with 0.1%–4% uncertainty) and models the respective uncertainties with Gaussian distributions. The muon pair final state search is significantly more powerful than the electron pair for $m > 212\,\mathrm{MeV}$ because its backgrounds are smaller. From the cross-section limits we derive limits on the Dark Photon coupling constant ϵ as a function of its mass m according to ref. [4]. Results are shown in fig. 4.

Bounds in the range $10^{-4} - 10^{-3}$ for $0.02 < m_{A'} < 10.2\ GeV$ are set, significantly improving previous constraints derived from beam-dump experiments [5-7], the electron anomalous magnetic moment [8], KLOE [9,10], WASA-at-COSY [11], HADES [12], A1 at MAMI [13], and the test run from APEX [14]. These results improve and supersede existing constraints obtained from a *BABAR* search for a light *CP*-odd Higgs boson [15,16] using a smaller dataset. We reduce the experimentally allowed parameter space that could explain with a Dark Photon the discrepancy between the calculated and measured anomalous magnetic moment of the muon [17].

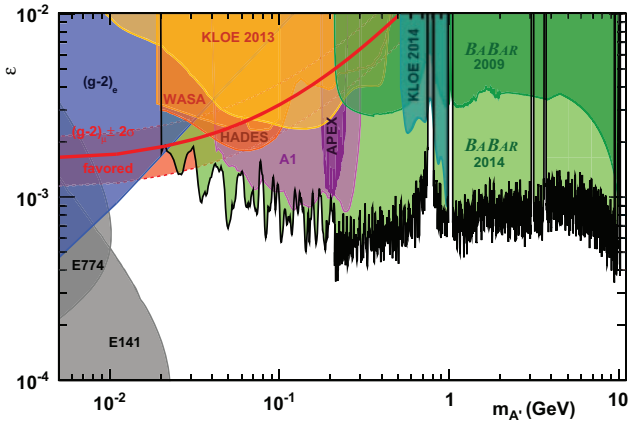

Fig. 4. – Upper limit (90% CL) on the mixing strength ϵ as a function of the dark photon mass. The values required to explain the discrepancy between the calculated and measured anomalous magnetic moment of the muon [17] are displayed as a red line.

3. – Search for long-lived particles in e^+e^- collisions

When NP particles are weakly coupled to standard matter, they can be long-lived if they are restricted to decay to SM particles [18]. Experiments have mostly searched for such long-lived particles at small masses under 1 GeV [6, 19, 20] and in the multi-GeV mass range [21-25]. The *BABAR* collaboration has completed a search that is sensitive to masses $\mathcal{O}$(GeV) [26].

We completed a model-independent search for inclusive production of a long-lived particle L in the process $e^+e^- \to LX$, where L decays at a displaced vertex into any of six different final states, $e^+e^-, \mu^+\mu^-, e^\pm\mu^\mp, \pi^+\pi^-, K^+K^-$ and $K^\pm\pi^\mp$. Except for 20 fb taken at the $\Upsilon(4S)$, which where used to test the analysis, we use the entire *BABAR* data collected at the $\Upsilon(4S)$, 40 MeV below the $\Upsilon(4S)$ peak, at the $\Upsilon(2S)$, and $\Upsilon(3S)$ corresponding to a luminosity of 489.1 fb.

We reconstruct L from two oppositely-charged tracks that originate from a common vertex with distance to the beam line in the transverse plane from 1 to 50 cm. The resolution on the radial distance must be smaller than 0.2 cm. We require that both tracks have impact parameters with respect to the beam line larger than 3 times the resolution. We reject background from K^0_S and Λ decays, and we skip searching on signal low-mass regions with problematic structures in the mass distribution by requiring, depending on the final state, that $m_{e^+e^-} > 0.44\,\text{GeV}$, $m_{\mu^+\mu^-} < 0.37\,\text{GeV}$ or $m_{\mu^+\mu^-} > 0.5\,\text{GeV}$, $m_{e^\pm\mu^\mp} > 0.48\,\text{GeV}$, $m_{\pi^+\pi^-} > 0.86\,\text{GeV}$, $m_{K^+K^-} > 1.35\,\text{GeV}$, and $m_{K^\pm\pi^\mp} > 1.05\,\text{GeV}$. According to a Monte Carlo simulation, surviving background consists primarily of hadronic events with high track multiplicity, where large-d_0 tracks originate mostly from K^0_S, Λ, $K^\pm$, and $\pi^\pm$ decays, as well as particle interactions with detector material. Random overlaps of such tracks comprise the majority of the background candidates.

We scan for a signal mass peak over a smooth background with an extended unbinned maximum likelihood fit with a polynomial background and a signal peak corresponding to a mass m whose shape and width we determine from a Monte Carlo simulation for 11 mass hypotheses. We repeat the fit in steps of 2 MeV. We determine the significance

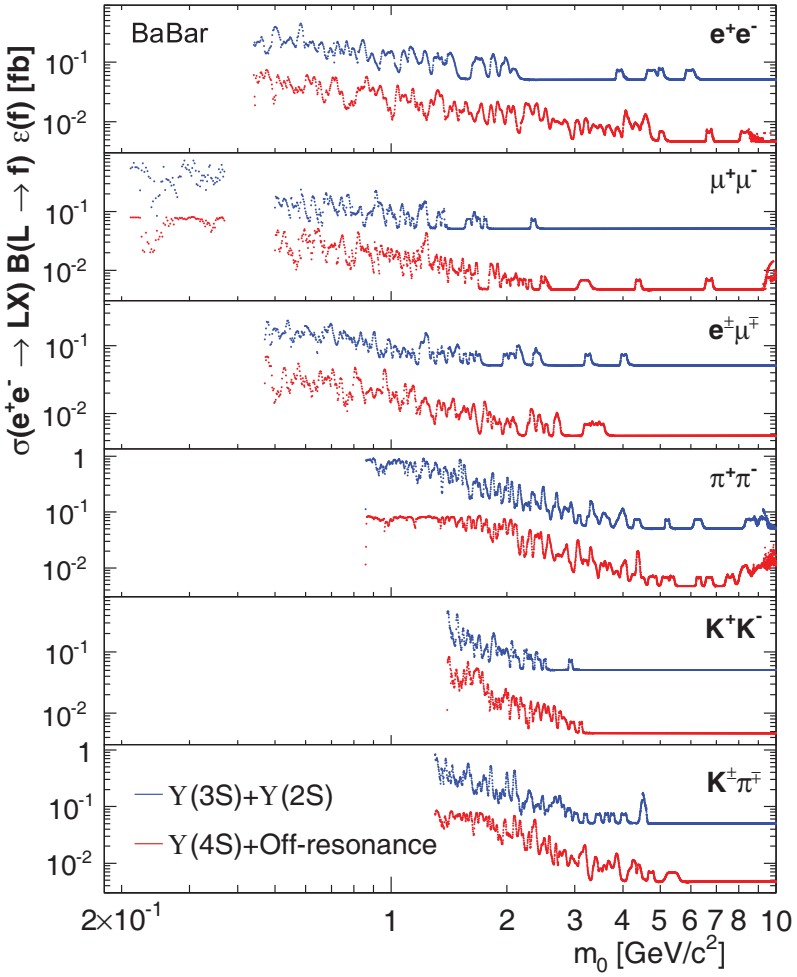

Fig. 5. – Upper limits on the cross section σ_f as a function of L mass for each final state (left) for $\Upsilon(4S)$ data (lower red curves) and for $\Upsilon(3S+\Upsilon(2S)$ data (upper blue curves) and on the product branching fraction $\mathcal{B}_{Lf}$ (right) for different decay lengths.

of the signal yield as $S = \sqrt{2\log(L/L_0)}$, where L and L_0 are the maximum-likelihood values for fits with and without freely varying signal, respectively.

For each final state mass scan, we determine the background-only hypothesis p-values of the largest found signal significances with positive signal yields using a large amount of background-only toy Monte Carlo simulations. No evidence of signal was found, hence we compute upper limits on the product $\sigma(e^+e^- \to LX)$ BF$(L \to f)$ $\epsilon(f)$ using the signal yield and the estimated *BABAR* integrated luminosity. We determine the signal yield profile likelihood using convolutions with Gaussians to account for systematic uncertainties on the signal efficiency (obtained from a Monte Carlo simulation) and on the background likelihood term. We obtain Bayesian 90% CL upper limits using a flat prior, shown in fig. 5.

For the purpose of testing specific NP models, the signal efficiency has been estimated with a Monte Carlo simulation using 11 L masses. The simulation used lifetime large

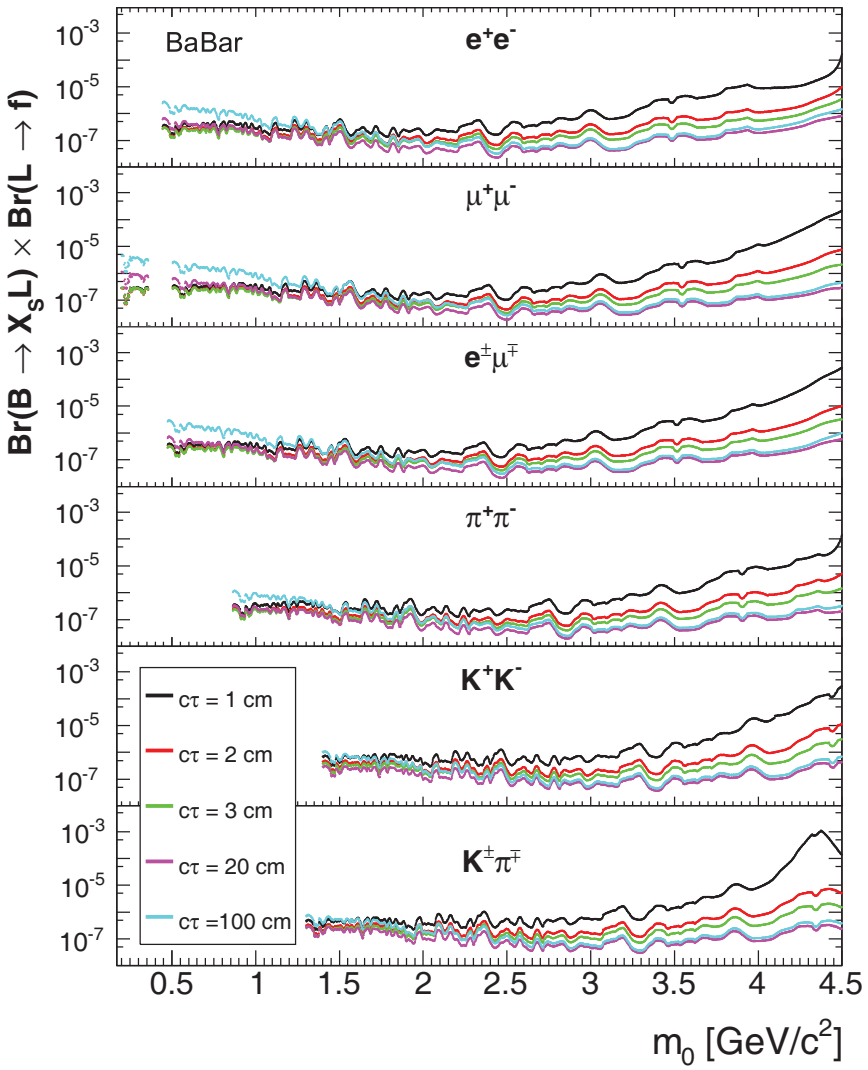

Fig. 6. – Upper limits on $\mathcal{B}_{Lf} = \mathcal{B}(B \to LX_s) \cdot \mathcal{B}(L \to f)$ as a function of the L mass for a selection of lifetimes.

enough to populate the acceptance in the radial distance of the displaced vertex. With appropriate weighting, also shorter lifetimes are then properly simulated. The estimated signal efficiencies as a function of the mass, the lifetime and the transverse momentum are provided to allow model testing [26].

We used the results to set constraints on a specific model where L is produced in B decays via $B \to LX_s$, where X_s is a hadronic state with strangeness $S = -1$ as in Higgs portal [27-30] and axion-portal [31] models of dark matter. By simulating the detection efficiency with this production model, we obtained limits on the product branching fraction $\mathcal{B}_{Lf} = \mathcal{B}(B \to LX_s) \cdot \mathcal{B}(L \to f)$, shown in fig. 6. These limits exclude a significant region of the parameter space of the inflaton model [27].

4. – Search for a light Higgs decaying to charm

The next-to-minimal supersymmetric standard model (NMSSM) [32, 33] provides an interesting solution to address some problematic issues of the minimal supersymmetric standard model (MSSM). The NMSSM has a rich Higgs sector with two charged, three neutral *CP*-even, and two neutral *CP*-odd bosons. The SM-like Higgs found at CERN [34, 35] is also consistent with one of the heavier neutral NMSSM Higgs bosons [36]. The lightest NMSSM Higgs A^0 may be produced at the B-factories and still have escaped the LEP searches [32, 37]. The *BABAR* collaboration has published light Higgs searches for a variety of decay modes. We report in the following the most recent search for A^0 production with masses ranging between 4.00 and 9.25 GeV followed by a decay to charm [38], which can be the dominant decay mode in this mass range for small values of the NMSSM parameter $\tan\beta$.

We analyze 13.6 fb^{-1} of data collected at the $\Upsilon(2S)$ resonance, corresponding to $(98.3 \pm 0.9) \times 10^6$ $\Upsilon(2S)$ mesons [39], which includes an estimated $(17.5 \pm 0.3) \times 10^6$ $\Upsilon(2S) \to \pi^+\pi^-\Upsilon(1S)$ decays [40]. We simulate the signal at 14 A^0 masses, and we simulate the backgrounds with resonant $e^+e^- \to \Upsilon(2S)$ and continuum $e^+e^- \to q\bar{q}$ events. For background subtraction, we use 1.4 fb^{-1} of "off-resonance" data collected 30 MeV below the $\Upsilon(2S)$ resonance.

We select events consistent with the decay chain $e^+e^- \to \Upsilon(2S) \to \pi^+\pi^-\Upsilon(1S)$, $\Upsilon(1S) \to \gamma A^0$, $A^0 \to c\bar{c}$ by requiring a pion pair, a photon and a reconstructed D from the A^0 decay. The D is recostructed as $D^0 \to K^-\pi^+$, $D^+ \to K^-\pi^+\pi^+$, $D^0 \to K^-\pi^+\pi^+\pi^-$, $D^0 \to K^0_S\pi^+\pi^-x$ and as $D^*(2010)^+ \to \pi^+D^0$ with $D^0 \to K^-\pi^+\pi^0$. The π^0 candidates are reconstructed from two photons, the K^0_S candidates are reconstructed from two oppositely charged pions. The photon must not be consistent with originating from a π^0 decay in association with another photon that is not used to reconstruct the D.

The mass of the system recoiling againts the di-pion must be consistent with the mass of the $\Upsilon(1S)$, and the A^0 invariant mass is determined from the mass of the system recoiling against the dipion and photon with $m^2_{A^0} = (P_{e^+e^-} - P_{\pi^+\pi^-} - P_\gamma)^2$. The four-momentum of the e^+e^- system in the center-of-mass frame is given by $P_{e^+e^-} = (M_{\Upsilon(2S)}, 0, 0, 0)$.

Backgrounds increase significantly with the A^0 masses, because the corresponding photon becomes softer, therefore the search is split and separately optimized in two mass regions, 4.00 to 8.00 GeV and 7.50 to 9.25 GeV. For each mass region and for each of the D channels we train a boosted decision tree with 24 variables using simulated signal and backgrounds data, in order to maximize $S/(1.5 + \sqrt{B})$ [41], where S and B are the expected numbers of signal and background events, respectively. We also use 5 variables of the di-pion system to determine a composite likelihood of signal and background di-pions on the simulation distributions, in order to improve the signal to background separation.

We select 9.8×10^3 and 7.4×10^6 candidates in the low- and high-mass regions, respectively. The backgrounds are $\Upsilon(1S) \to \gamma gg$, other $\Upsilon(1S)$ decays, $\Upsilon(2S)$ decays without a dipion transition, and $e^+e^- \to q\bar{q}$ events. We perform an extended maximum likelihood fit of a A^0 mass peak over smooth second-order polynomial background. The signal peak is modeled with a Crystal Ball function [42]. The signal shape is fixed by interpolating simulations from the two closest A^0 masses, while the background is fit on data. We scan in steps of 10 and 2 MeV for the low- and high-mass regions, respectively. The step sizes are at least 3 times smaller than the mass resolution. We do not perform

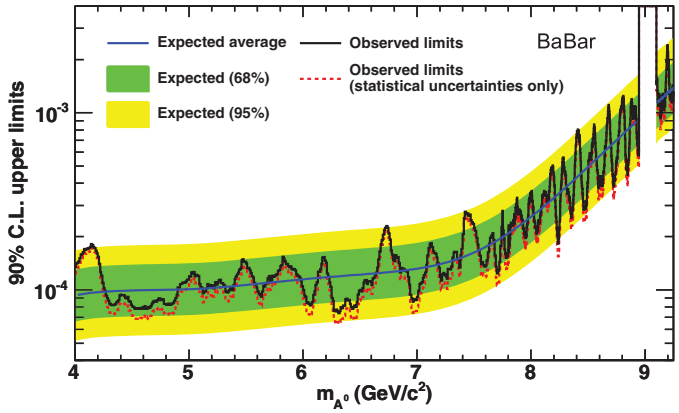

Fig. 7. – The 90% CL upper limits on the product branching fraction $\mathcal{B}(\Upsilon(1S) \to \gamma A^0) \times \mathcal{B}(A^0 \to c\bar{c})$ using all uncertainties (thick line) and using statistical uncertainties only (thin dashed line). The inner and outer bands contain 68% and 95% of our expected upper limits. The bands are calculated using all uncertainties. The thin solid line in the center of the inner band is the expected upper limit.

a fit for $8.95 < m_{A^0} < 9.10\,\text{GeV}$ because of a large background from $\Upsilon(2S) \to \gamma\chi_{bJ}(1P)$, $\chi_{bJ}(1P) \to \gamma\Upsilon(1S)$ decays.

We detemine from the simulation of pseudo-experiments the statistical significance of the largest signal yields and we do not find evidence for signal. We compute Bayesian 90% CL upper limits on the product branching fraction $\mathcal{B}(\Upsilon(1S) \to \gamma A^0) \times \mathcal{B}(A^0 \to c\bar{c})$ assuming a uniform prior, with the constraint that the product branching fraction be greater than zero. The distribution of the likelihood function for N_{sig} is assumed to be Gaussian with a width equal to the total uncertainty in N_{sig}, including systematic uncertainties. The results are shown in fig. 7.

5. – Search for π^0-like particles coupled to the τ-lepton

The *BABAR* measurement of the π^0 transition form factor in two-photon collisions [43] exceeds the Brodsky-Lepage limit of $\sqrt{2}f_\pi/Q^2 \simeq 185\ \text{MeV}/Q^2$ [44], which is expected to hold at high transferred momentum, where perturbative QCD should provide a reliable prediction. The corresponding Belle measurement [45] is consistent both with the perturbative prediction and with the *BABAR* result (see fig. 8). The discrepancy in the *BABAR* measurement may be explained with the ad-hoc hypothesis of a π^0-like particle with a specific coupling to the tau [46]. The new particle ϕ can be a pseudoscalar ϕ_{P} that does not mix appreciably with the π^0, a pseudoscalar that mixes with the π^0 into a so-called hardcore-pion π^0_{HC} or a scalar particle ϕ_{S}. We test this model by searching for evidence of ϕ in associated production with a τ-lepton pair in the process $e^+e^- \to \tau^+\tau^-\phi$ using the $\Upsilon(4S)$-peak *BABAR* data sample ($468\,\text{fb}^{-1}$, corresponding to 4.3×10^8 τ pairs) [47]. A large and significant signal is expected in order to explain the π^0 transition form factor discrepancy.

We select events with a final state containing an electron, a muon and two photons, corresponding to the production of a tau pair and a ϕ, where one τ decays to $e\bar{\nu}_e\nu_\tau$, the

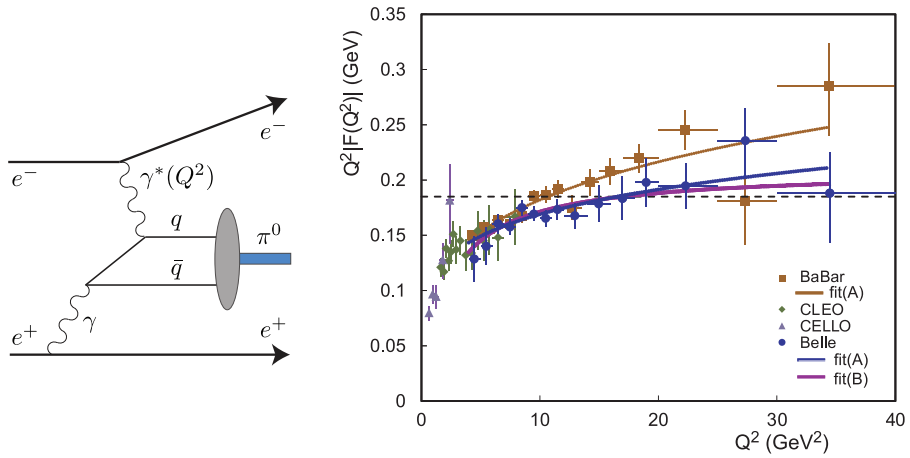

Fig. 8. – Left: graph for π^0 production in two-photon interactions where one photon is about real and the other one virtual. Right: π^0 transition form factor measurements *vs.* the Brodsky-Lepage limit.

other one to $\mu\bar{\nu}_\mu\nu_\tau$ and the ϕ decays as a π^0 into two photons. To suppress background we require $2.2 < E_\phi < 4.7\,\text{GeV}$ in the laboratory frame, a minimum photon energy in the laboratory of 0.25 GeV and a sizeable angle between the photons and the beams. Large background from standard model τ decays is effectively suppressed by requiring that the invariant mass of the ϕ and each of the tracks be larger than the τ mass and that the sum of the energy of the ϕ and of each of the tracks be larger than half the event energy in the center of mass reference system. Finally, the event must not have additional neutral energy larger than 300 MeV in the laboratory frame.

We perform an extended unbinned maximum-likelihood fit on the mass distribution of the ϕ candidates from 50 to 300 MeV with a model including a Gaussian for the signal and a Gaussian for the expected peaking background of π^0's on top of a first degree polynomial non-peaking background. The Gaussian widths are fixed from fits on control samples of π^0's obtained by reversing part of the selection requirements. The peaking background normalization is determined with the simulation. We fix the ϕ mass in steps of $0.5\,MeV$ (less that half the mass resolution) and we get the maximum signal yield in its predicted mass range from 110 to 160 MeV. The backgrounds-subtracted signal yield is $5.0 \pm 2.7 \pm 0.4$. Peaking backgrounds from e^+e^- annihilation events and from two-photon events are estimated with simulation to be 0.38 ± 0.09 and 1.24 ± 0.37 events, respectively.

To obtain the production cross-section $\sigma(e^+e^- \to \tau^+\tau^-\phi)$ we determine the signal selection efficiency with simulation. Factoring out the $\tau^- \to \mu^-\overline{\nu}_\mu\nu_\tau$ and the $\tau^- \to e^-\overline{\nu}_e\nu_\tau$ branching fractions, the efficiencies are found to be $\varepsilon(\phi_{\rm P}) = \varepsilon(\pi^0_{\rm HC}) = (0.455 \pm 0.017)\%$ and $\varepsilon(\phi{\rm S}) = (0.0896 \pm 0.0033)\%$. The efficiency to reconstruct the scalar ϕ is smaller than that to reconstruct the pseudoscalar one because scalar particles are preferentially produced with small energy and fail the requirements on the track-ϕ invariant mass and sum of energy.

Systematic uncertainties are estimated by comparing data and simulation control samples to account for imperfections in modeling the energy scale and resolution of track momenta and photon energy reconstruction, the π^0 reconstruction efficiency, the particle identification and the signal efficiency.

TABLE I. – *Consistency (p-value) of the theory model when fitting both the BABAR π^0 transition form factor excess and the π^0-like particles' production cross-section $\sigma(e^+e^- \to \tau^+\tau^-\phi)$.*

Model	$\Delta\chi^2$/n.d.f.	p-value
$\pi^0_{\rm HC}$	11.8/1	5.9×10^{-4}
$\phi_{\rm P}$	37.6/1	8.8×10^{-10}
$\phi_{\rm S}$	35.8/1	2.2×10^{-9}

Using signal efficiency and the estimated systematic uncertainties we measure the signal cross-sections:

$$\sigma = \begin{cases} 38 \pm 21(\text{stat}) \pm 3(\text{syst})\,\text{fb} & \text{for } \phi_{\rm P} \text{ and } \pi^0_{\rm HC}, \\ 190 \pm 100(\text{stat}) \pm 20(\text{syst})\,\text{fb} & \text{for } \phi_{\rm S}. \end{cases}$$

In order to test the validity of the model that would account for the *BABAR* π^0 transition form factor discrepancy with respect to the Brodsky-Lepage limit, we perform the χ^2 fit for the best coupling constants that match the *BABAR* transition form factor result with the addition of a χ^2 term that accounts for the coupling constant constraint that corresponds to the above cross-section measurements. The increase in χ^2 after adding the constraint follows a χ^2 distribution with one degree of freedom, which we use to get the p-values on the NP model consistency with the data. The results are reported in table I and all three hypotheses are ruled out with very small probabilities of statistical consistency.

6. – Conclusion and outlook

The clean and large e^+e^- collision samples collected by *BABAR* have been used to search for a variety of light New Physics particles, without finding evidence for any signal, and providing significant experimental constraints to present and future theory models.

No dark photon has been found in the 0.02–10.2 GeV mass region, constraining the mixing parameter ϵ to be less than 10^{-4} to 10^{-3} depending on the dark photon mass. We do not find evidence of long-lived particle in the $0.2 < m < 10$ GeV mass range and proper decay lengths of $0.5 < c\tau < 100$ cm and we published appropriate 90% CL upper limits on the product $\sigma(e^+e^- \to LX) \cdot \mathcal{B}(L \to f) \cdot \epsilon_f$. We extended previous searches for a light Higgs produced in Υ decays to the case where the light Higgs decays to a final state with charm, setting significant constraints on the parameter space of NMSSM models. Finally, we searched for the production of π^0-like particles in association with a $\tau^+\tau^-$ pair and we rule out with high confidence New Physics models that have been proposed to account for the experimental excess observed by *BABAR* on the measurement of the π^0 transition form factor in two-photon events.

Belle has collected about twice the amount of *BABAR* events, and has good prospects of improving part of the above measurements. BelleII with 50 ab^{-1} and an improved trigger for light New Physics searches will be able to ameliorate all the presented limits by one order of magnitude or more.

REFERENCES

[1] Essig R., Jaros J. A., Wester W., Adrian P. H., Andreas S. *et al.*, *Working Group Report: New Light Weakly Coupled Particles* (2013).
[2] Holdom B., *Phys. Lett. B*, **166** (1986) 196.
[3] Lees J. P. *et al.*, *Phys. Rev. Lett.*, **113** (2014) 201801.
[4] Pospelov M., Ritz A. and Voloshin M. B., *Phys. Lett. B*, **662** (2008) 53.
[5] Blumlein J. and Brunner J., *Phys. Lett. B*, **701** (2011) 155.
[6] Andreas S., Niebuhr C. and Ringwald A., *Phys. Rev. D*, **86** (2012) 095019.
[7] Blmlein J. and Brunner J., *Phys. Lett. B*, **731** (2014) 320.
[8] Endo M., Hamaguchi K. and Mishima G., *Phys. Rev. D*, **86** (2012) 095029.
[9] Babusci D. *et al.*, *Phys. Lett. B*, **720** (2013) 111.
[10] Babusci D. *et al.*, *Phys. Lett. B*, **736** (2014) 459.
[11] Adlarson P. *et al.*, *Phys. Lett. B*, **726** (2013) 187.
[12] Agakishiev G. *et al.*, *Phys. Lett. B*, **731** (2014) 265.
[13] Merkel H., Achenbach P., Ayerbe Gayoso C., Beranek T., Bericic J. *et al.*, *Phys. Rev. Lett.*, **112** (2014) 221802.
[14] Abrahamyan S. *et al.*, *Phys. Rev. Lett.*, **107** (2011) 191804.
[15] Aubert B. *et al.*, *Phys. Rev. Lett.*, **103** (2009) 081803.
[16] Bjorken J. D., Essig R., Schuster P. and Toro N., *Phys. Rev. D*, **80** (2009) 075018.
[17] Pospelov M., *Phys. Rev. D*, **80** (2009) 095002.
[18] Schuster P., Toro N. and Yavin I., *Phys. Rev. D*, **81** (2010) 016002.
[19] Gninenko S. N., *Phys. Rev. D*, **85** (2012) 055027.
[20] Adams T. *et al.*, *Phys. Rev. Lett.*, **87** (2001) 041801.
[21] Abazov V. M. *et al.*, *Phys. Rev. Lett.*, **97** (2006) 161802.
[22] Abe F. *et al.*, *Phys. Rev. D*, **58** (1998) 051102.
[23] Aad G. *et al.*, *Phys. Lett. B*, **720** (2013) 277.
[24] Aad G. *et al.*, *Phys. Rev. Lett.*, **108** (2012) 251801.
[25] Aad G. *et al.*, *Phys. Lett. B*, **719** (2013) 280.
[26] Lees J. P. *et al.*, *Phys. Rev. Lett.*, **114** (2015) 171801.
[27] Bezrukov F. and Gorbunov D., *JHEP*, **1307** (2013) 140.
[28] Cheung C. and Nomura Y., *JHEP*, **11** (2010) 103.
[29] Schmidt-Hoberg K., Staub F. and Winkler M. W., *Phys. Lett. B*, **727** (2013) 506.
[30] Clarke J. D., Foot R. and Volkas R. R., *JHEP*, **02** (2014) 123.
[31] Freytsis M., Ligeti Z. and Thaler J., *Phys. Rev. D*, **81** (2010) 034001.
[32] Dermisek R., Gunion J. F. and McElrath B., *Phys. Rev. D*, **76** (2007) 051105.
[33] Maniatis M., *Int. J. Mod. Phys. A*, **25** (2010) 3505.
[34] Aad G. *et al.*, *Phys. Lett. B*, **716** (2012) 1.
[35] Chatrchyan S. *et al.*, *Phys. Lett. B*, **716** (2012) 30.
[36] Christensen N. D., Han T., Liu Z. and Su S., *JHEP*, **1308** (2013) 019.
[37] Wilczek F., *Phys. Rev. Lett.*, **39** (1977) 1304.
[38] Lees J. *et al.*, *Phys. Rev. D*, **91** (2015) 071102.
[39] Lees J. P. *et al.*, *Nucl. Instrum. Meth. A*, **726** (2013) 203.
[40] Olive K. A. *et al.*, *Chin. Phys. C*, **38** (2014) 090001.
[41] Punzi G., *eConfC*, **030908** (2003) MODT002, [79(2003)].
[42] Oreglia M., *A Study of the Reactions* $\psi' \to \gamma\gamma\psi$, Ph.D. thesis, SLAC (1980) `http://www-public.slac.stanford.edu/sciDoc/docMeta.aspx?slacPubNumber=slac-r-236.html`.
[43] Aubert B. *et al.*, *Phys. Rev. D*, **80** (2009) 052002.
[44] Brodsky S. J., Lepage G. P. and Mackenzie P. B., *Phys. Rev. D*, **28** (1983) 228.
[45] Uehara S. *et al.*, *Phys. Rev. D*, **86** (2012) 092007.
[46] McKeen D., Pospelov M. and Roney J. M., *Phys. Rev. D*, **85** (2012) 053002.
[47] Lees J. P. *et al.*, *Phys. Rev. D*, **90** (2014) 112011.